

e^N TRANSITION PREDICTION FOR 3D WING CONFIGURATIONS USING DATABASE METHODS AND A LOCAL, LINEAR STABILITY CODE

Andreas Krumbein*

*Deutsches Zentrum für Luft- und Raumfahrt e.V. – DLR (German Aerospace Center)
Institute of Aerodynamics and Flow Technology, Numerical Methods
Bunsenstr. 10, D-37073 Göttingen, Germany
e-mail: andreas.krumbein@dlr.de

Key Words: Transition prediction, RANS solver, e^N -method, 3D wings

Abstract: *A Reynolds-averaged Navier-Stokes solver, a laminar boundary-layer code and different transition prediction methods for the prediction of Tollmien-Schlichting and cross flow instabilities were coupled in order to perform Reynolds-averaged Navier-Stokes computations of three-dimensional, finite wings with automatic laminar-turbulent transition prediction. The results from computations based on two database methods and a local, linear stability code together with the e^N -method are compared for a three-dimensional wing configuration.*

1. INTRODUCTION

The modelling of laminar-turbulent transition in Reynolds-averaged Navier-Stokes (RANS) solvers is a crucial issue when high quality simulation results for aircraft shall be produced. Especially the simulation of flows around high-lift systems of aircraft may result in significant errors when the transition points are of insufficient accuracy or are not taken into account at all. High-lift systems very often involve multi-component wings (e.g. slat, main wing, and flaps) and may have very high levels of total circulation. Because all components of the high-lift system are in close interaction with one another the total circulation and the complete flow field is affected by one transition line on one of the components.

Although the overall lift value may be predicted with satisfactory accuracy slight deviations between the real and the computed pressures can lead to large errors in the computed overall drag value. This issue was investigated in detail in [1] and it was shown that the overall pressure drag of a high-lift configuration, which dominates the drag value of the configuration as a whole as well as the drag of every single element, is composed of a balance of very large positive and negative contributions. The contribution of one single element may be one order of magnitude larger than the resulting overall drag of the complete configuration. Thus, a relative error of 5% of the computed drag on the slat upper side may result in a change of 50% for the overall drag value.

For the design process of wings in industry, there exists the demand for a RANS-based computational fluid dynamics (CFD) tool that is able to handle flows automatically and autonomously with laminar-turbulent transition. Existing transition prediction methods vary from empirical transition criteria via the local, linear stability equations based on small disturbance theory or non-local, linear and non-local, non-linear stability methods using the parabolized stability equations over large eddy simulations to direct numerical simulations of the Navier-Stokes equations. Empirical transition criteria and the e^N -method [2],[3] based on local, linear stability theory and the parallel flow assumption represent *state-of-the-art* methods for the prediction of transition onset in many industrial applications. Although they do not account for a number of fundamental aspects in the transition process e^N -methods are used in aircraft industry most frequently for design purposes covering transition due to Tollmien-Schlichting (TS) and cross flow (CF) instabilities. Because there are no other practical methods presently available for industrial applications [4] e^N -methods together with the two- N -factor method and empirical criteria for transition mechanisms which are not covered by the e^N approach (e.g. bypass and attachment line transition) are going to be used

further on for the design of aircraft wings and wing systems even for a future laminar wing of transport type aircraft.

The first steps towards the setup of a RANS-based CFD tool with automatic transition prediction were made, for example, in [5], where a RANS solver and an e^N -method were applied and in [6], where a RANS solver, a laminar boundary-layer method [7], and an e^N -method were coupled. There, the boundary-layer method was used to produce highly accurate laminar, viscous layer data to be analyzed by a linear stability code. Hence, the very expensive grid adaptation necessary to produce accurate viscous layer data directly from the Navier-Stokes grid was avoided. The use of e^N -database methods [8],[9] results in a coupled program system that is able to handle transition prediction automatically. In [10] a database for the growth rates is used which are represented by a trained neural network based on Falkner-Skan-Cooke profiles. Alternative approaches using a transition closure model or a transition/turbulence model directly incorporated into the RANS solver are documented in [11]-[13]. A correlation-based transition modelling approach built on local variables using transport equations for the intermittency and for a transition onset criterion in terms of the momentum thickness Reynolds number is documented in [14].

At the Deutsches Zentrum für Luft- und Raumfahrt, German Aerospace Center (DLR), the block structured RANS code FLOWer [15] is used together with the laminar boundary-layer method in [7] and the e^N -database methods in [8] and [9]. The laminar boundary-layer method and the e^N -database methods form a so called 'transition prediction module' that is coupled to the RANS solver and that interacts with the RANS solver during the computation [16],[17]. Presently, the transition prediction module of FLOWer can be applied to two-dimensional one-element or multi-element configurations and to three-dimensional one-element or multi-element wing configurations.

The main objective of this paper is to point out a severe problem which can arise when transition prediction tools based on the e^N -method are applied to configurations tested in a wind tunnel. Here, a shortcoming of the e^N -method plays a crucial role. This shortcoming is inherent in the e^N -method because it is a semi-empirical method which requires the knowledge of the N factors. The N factors have to be determined experimentally, and for wings of transport type aircraft in free flight the ranges of values of the N factors for TS and CF instabilities were determined in extensive flight test programs. This fact justifies the application of the e^N -method when free flight configurations are investigated numerically. For wind tunnel flows, however, the N factors must be determined individually for each wind tunnel because their values depend on the specific characteristics of the wind tunnel. Here, difficulties can arise – especially in the case of CF instabilities – when the N factors are not known. These difficulties become particularly obvious when validation work must be realized based on experimental test cases which lack sufficient information necessary for the transition prediction or when the experimental data are not clearly interpretable or even contradictory. In these cases, the e^N -method must be calibrated using transition information from the experiment itself.

Up to now it was necessary to use transition database methods in order to apply the e^N -method for transition prediction in a fully automatic way so that the transition location iteration could be executed without intervention (automatic) by the user of the RANS code and without *a priori* knowledge of the transition characteristics of the specific flow problem (autonomous). Now a fully automated local, linear stability solver [18] is available using a frequency estimator for the detection of the relevant regions of amplified disturbances for TS instabilities and a wave length estimator for CF instabilities. The new stability solver is currently incorporated into the FLOWer transition prediction module.

In this work the new stability solver is applied to a three-dimensional wing configuration, the transition locations are determined using the e^N -method and the results are compared with results from the e^N -database method for TS instabilities and the e^N -database method for CF instabilities. The comparison and assessment is done in terms of the maximum N factor curves for TS and CF waves based on the two different approaches. Special emphasis is given to the values of the critical N factors N_{TS}^* and N_{CF}^* and the N_{CF} - N_{TS} stability boundary.

2. TRANSITION PREDICTION COUPLING

The coupled program system consists of the RANS solver itself [15], a laminar boundary-layer method for swept, tapered wings [7] and different transition prediction methods, which are provided with all necessary data by the laminar boundary-layer method. The laminar boundary-layer method solves the compressible laminar boundary-layer equations for conical external flow using the surface pressure distribution from the stagnation or attachment line point along a wing section as input.

The RANS solver communicates the surface pressure distribution of the configuration as input data to the laminar boundary-layer method, the laminar boundary-layer method computes all of the boundary-layer parameters that are needed for the transition prediction method and the transition prediction method determines new transition locations that are given back to the RANS solver. This coupled structure results in an iterative procedure for the transition locations within the iteration of the RANS equations [19],[20]. The structure of the approach is outlined graphically in Fig. 1 (where lam. bl is the laminar boundary layer).

During the computation, the RANS solver is stopped after a certain number of iteration cycles k usually when the lift has sufficiently converged, that is when pressure oscillations have been damped to a sufficiently low degree. Then the transition module is called and first the surface pressure distribution $c_p(\text{cycle} = k)$ along a wing section is used as input for the boundary-layer code. All viscous data – basically the velocity profiles in streamwise and crossflow direction and their 1st and 2nd derivatives – are calculated by the boundary-layer code. Then, the transition prediction method analyzes the laminar boundary layer and tries to determine a transition point which is located upstream of the separation point predicted by the boundary-layer code. If a transition point due to TS or CF instabilities was found it is communicated back to the RANS solver. If no transition point due to TS or CF instabilities upstream of the laminar separation point could be found the laminar separation point is used as approximation of the real transition point. This is an attempt to predict transition due strictly to the presence of separation bubbles. This approach often yields a good approximation of the real transition point when transition does not occur before the laminar boundary layer separates, particularly for low Reynolds number flows. These steps are done for the upper and lower sides of all specified wing sections. When all new transition locations, $x_j^T(\text{cycle} = k)$ with $j = 1, \dots, n_T$, where n_T is the number of transition points, have been communicated back to the RANS solver, each transition location is slightly underrelaxed to damp oscillations in the convergence history of the transition locations. Then, all underrelaxed transition points – they represent a transition line on the upper or lower surface of a wing element in form of a polygonal line – are mapped into the surface grid of the configuration applying a transition setting algorithm [16] subdividing the surface of the geometry into laminar and turbulent regions, and the computation is continued. In so doing, the determination of the transition locations becomes an iteration process itself. With each transition location iteration step the underrelaxation factor is reduced until a converged state of all transition points has been obtained. A wing section is approximated by a chordwise surface grid line of the block-structured grid.

3. COMPUTATIONAL RESULTS

In [20] computational results for the ONERA M6 wing [21] obtained with the transition prediction coupling procedure for the aerodynamic parameters $M_\infty = 0.262$ and $Re_\infty = 3.5 \times 10^6$

are shown. There, these results are compared to the experimental findings reported in [22] which presents the outcome of experiments carried out in the ONERA S2Ch (Chalais-Meudon) wind tunnel for which a turbulence intensity of $Tu_\infty = 0.2\%$ is given. In the experiments the laminar regions were detected and visualized applying a sublimation technique based on naphthalene.

Here, this configuration was computed using the Baldwin-Lomax turbulence model [23] and the two e^N -database methods using Mack's relationship $N^* = -8.43 - 2.4 \ln(Tu_\infty)$ for the two critical N factors $N_{TS}^* = N_{CF}^* = 6.485$. The transition points were determined in three wing sections, $\eta = 0.22, 0.42, 0.86$. In [22] the development of the transition points on upper and lower sides of the wing are given in a diagram for the angles of attack $\alpha = 0^\circ, 5^\circ, 10^\circ$, and 15° for the wing section at $\eta = 0.45$ (for which most experimental transition information is available) and compared here with the results obtained for $\eta = 0.42$ which corresponds to the grid line nearest to $\eta = 0.45$, Fig. 2. On the upper side of the wing all transition locations are due to laminar separation, that is, all transition points were approximated by laminar separation points from the boundary-layer code. On the lower side of the wing all transition points are due to CF instabilities according to the CF database method. The comparison of the computed and experimental results shows clear deviations from one another. The deviations on the upper side are an indication that approximating transition points by laminar separation points can lead to errors which can be eliminated when criteria for the prediction of transition inside laminar separation bubbles [24] are applied which yield a transition point downstream of the point of laminar separation instead of using the separation point itself. The incorporation of criteria for this transition mechanism into the transition prediction module is one of the next development steps for the transition prediction module. The deviations on the lower side can be explained with an inappropriate setting of the values of the critical N factors N_{TS}^* and N_{CF}^* . This issue is addressed next.

Especially the unacceptable deviation on the lower side for $\alpha = 5^\circ$ requires an investigation of the N factor curves for this angle of attack which are shown in Fig. 3. For the three wing sections the N factor curves for TS and CF instabilities are shown. It can be seen that in the inboard section (Sec. 1) and the outboard section (Sec. 3) TS instabilities and in the midboard section (Sec. 2) a CF instability lead to transition when $N_{TS}^* = N_{CF}^* = 6.485$ is applied. Especially the setting $N_{CF}^* = 6.485$ is inappropriate because Mack's relationship is valid only for TS transition.

In order to find an appropriate value for N_{CF}^* experimental information from [25] for the S2Ch wind tunnel were used and the attempt was made to derive the stability boundary, Fig. 4. The stability boundary is defined by four points in the N_{CF} - N_{TS} plane and by a curve which approximates the region of mixed (TS and CF dominated) transition. The four points are given by the two critical N factors N_{TS}^* and N_{CF}^* on the one hand and by the values which mark the endings of the regions of purely TS dominated or CF dominated transition and thus define the initial and end points of the mixed transition region, N'_{TS} and N'_{CF} , on the other hand. In [25] the values $N_{TS}^* = 7.0$, $N_{CF}^* = 6.0$, $N'_{TS} = 3.5$ and $N'_{CF} = 5.5$ – these values correspond to the coordinate pairs (0.0, 7.0), (3.5, 7.0), (6.0, 5.5) and (6.0, 0.0) in the N_{CF} - N_{TS} plane – and a linear curve for the approximation of the mixed transition region (stability boundary No. 1) are used. In the transition prediction module which is used with the FLOWer code the region of mixed transition is approximated by the quarter of an ellipse leading to stability boundary No. 2 in Fig. 4 based on the same values for N_{TS}^* , N_{CF}^* , N'_{TS} and N'_{CF} . Using $N_{TS}^* = 6.485$ according to Mack's relationship and $N_{CF}^* = 5.75$ omitting the experimental data point at (≈ 7.0 , ≈ 2.0) leads to stability boundary No. 3. All these three stability boundaries are equivalent because the very limited amount of experimental information for the stability boundary makes a clear decision impossible.

As can be seen, none of these three stability boundaries leads to a significantly better result from the computation. According to the $N_{CF}-N_{TS}$ curve along the mid wing section of this flow case in Fig. 4 transition is purely CF dominated and to obtain the experimentally detected transition location $(x_7/c)_{sec} \approx 0.34$ on the lower side in the mid wing section at $\alpha = 5^\circ$ a value of $N_{CF}^* \approx 5.16$ is required. It is very probable that the naphthalene sublimation technique has strongly affected the CF transition process and accelerated transition. Using the value $N_{CF}^* \approx 5.16$ which was calibrated for one angle of attack ($\alpha = 5^\circ$) the computations for $\alpha = 5^\circ, 10^\circ$, and 15° were repeated leading to the results shown in Fig. 5. On the lower side of the mid wing section all computed transition points especially those for $\alpha = 10^\circ$ and 15° are of good accuracy.

In [20] it was shown that it is necessary also to calibrate N_{TS}^* in order to obtain good results for the transition lines over the whole span of the M6 wing for all angles of attack. Very probably also the TS transition was accelerated by the naphthalene sublimation technique. Calibrating the critical TS N factor using $N_{TS}^* = 4.75$ for the TS database method – the calibration was done using the experimental transition location on the lower side in the wing section $\eta = 0.96$ from $\alpha = 5^\circ$ – yields the expected improvements and leads to the stability boundary No. 4 in Fig. 4 when the values for N_{TS}^* and N_{CF}^* are kept as before, $N_{TS}^* = 3.5$ and $N_{CF}^* = 5.5$.

If the assumption is true that the naphthalene sublimation technique has influenced the transition process it is clear that it is not possible to obtain correct transition prediction results using transition data from other experiments which did not suffer from the same influence. Thus, in the case that validation work for transition prediction methods has to be carried out using a specific test case it can happen that the calibration of the TS and CF N factors is the only way possible to execute the task.

The computation of the N factor curves for TS and CF instabilities for $\alpha = 5^\circ$ in the three wing sections $\eta = 0.22, 0.42, 0.86$ using the local, linear stability solver LILO [18] yields the results depicted in Fig. 6 where the three curves are compared with the results from the two database methods. While the N factor curves for TS instabilities based on the two different approaches are very close to each other the N factor curves for CF instabilities differ significantly. Along the complete chord of the wing section the slopes of all three CF N factor curves from the stability code are much lower than those from the CF database method leading to much lower N factor values. Over a wide range of the chord the stability code N factors are more or less half as big as those from the database method. Beyond the chordwise position $(x/c)_{sec} \approx 0.6$ all curves from the stability code tend smoothly to lower values while the curves from the database method show a wiggly behaviour. The global shape of the corresponding curves for the three wing sections is very similar for the two different approaches. Also the gap between the curves for Sec. 1 and Sec. 3 on the one hand and the curve for Sec. 2 on the other hand occurs in the results of both approaches.

The differences in the CF N factor curves are essentially due to the different integration strategies used for the calculation of the CF N factor value at a certain surface point of the wing section specified by a chordwise position x_{sec} . While for the computation of the TS N factor N_{TS} the integration strategy is the same in the TS database method and in the LILO code namely

$$N_{TS}(x_{sec}) = \max_f \left(\int_{x_{sec}^0}^{x_{sec}} -\alpha_i(f; x_{sec}) dx_{sec} \right) \quad (1)$$

(with the local spatial amplification rate α_i , the frequency f and the neutral-point location x_{sec}^0 , where $\alpha_i(f; x_{\text{sec}}^0) = 0$) for which the integration is carried out in the direction of the inviscid stream line taken as wave propagation direction, for the CF N factor N_{CF} different integration strategies are applied in the CF database method and in the LILO code. The CF database method uses

$$N_{\text{CF}}(x_{\text{sec}}) = \max_{\Psi} \left(\max_f \left(\int_{x_{\text{sec}}^0}^{x_{\text{sec}}} -\alpha_i(f, \Psi; x_{\text{sec}}) dx_{\text{sec}} \right) \right), \quad (2)$$

the maximum value out of all available N factor values from the set of curves given by the parameters f and Ψ , which denotes the wave propagation direction. Because $f \neq 0$ in the integration strategy the CF database method is suited for instationary (travelling) CF waves. In the LILO code

$$N_{\text{CF}}(x_{\text{sec}}) = \max_{\lambda} \left(\int_{x_{\text{sec}}^0}^{x_{\text{sec}}} -\alpha_i(f=0, \lambda; x_{\text{sec}}) dx_{\text{sec}} \right) \quad (3)$$

is applied using the wave length λ as parameter for stationary CF waves ($f = 0$).

Both travelling and stationary CF waves can be present and lead to CF dominated transition depending on the flow environment. It is commonly accepted that travelling CF waves trigger transition in a high disturbance environment, whereas stationary CF waves dominate CF transition in a low disturbance environment. The former are excited by free stream turbulence and the latter by micronized surface roughness [25]-[28]. The turbulence intensity value $Tu_{\infty} = 0.15\%$ is often given as threshold between low disturbance and high disturbance environment, but experimentally it was found that in the range $0.1\% \leq Tu_{\infty} \leq 0.3\%$ one can not be sure about which type of CF transition actually occurs [28].

In Fig. 7 the different $N_{\text{CF}}-N_{\text{TS}}$ curves along the mid wing section for the two approaches and the corresponding $(x/c)_{\text{sec-over-}N_{\text{CF}}}$ curves are depicted. Calibrating the CF N factor using the value which corresponds to the transition location from the experiment $(x_T/c)_{\text{sec}} \approx 0.34$ yields $N_{\text{CF}}^* \approx 2.86$ and shows that also here transition is purely CF dominated. Keeping the values $N_{\text{TS}}^* = 3.5$ and $N_{\text{CF}}^* = 5.5$ as before lets the corresponding stability boundary degenerate to a rectangle (stability boundary No. 5). This is an inaccurate representation of the stability boundary and can lead to errors in the simulation.

Because RANS-based CFD tools with automatic transition prediction are applied to many different flow configurations, for example, to aircraft in free flight with a low disturbance environment or to models in wind tunnels tested in a high disturbance environment, it is advantageous to have different transition prediction tools at hand which, as a whole, cover all transition mechanisms which can occur in practical applications, especially those which are common in different branches of industry. For the practical application of transition prediction tools based on the e^N -method it is necessary to have sufficient experimental transition data at hand, so that the stability boundary for the transition prediction can be derived. For the determination of the stability boundary it is necessary to know at least four values, N_{TS}^* , N_{CF}^* , N_{TS}' , and N_{CF}' , which, in principle, must be derived for every particular integration strategy using the same experimental data. This means that higher efforts, experimentally as well as computationally, must be undertaken when model configurations with transition are to be investigated in order to have full benefit of the transition prediction tools which are currently available. From a validation point of view it is necessary to satisfy this requirement because

otherwise it is not possible to use the complete range of the simulation capabilities which can be provided.

4. CONCLUSIONS

Two e^N -database methods and a linear stability code were used to calculate the maximum N factor curves for TS and CF waves and transition locations for a three-dimensional wing configuration. The results of the different approaches were compared. Special emphasis was given to the values of the critical N factors N_{TS}^* and N_{CF}^* and the $N_{CF}-N_{TS}$ stability boundary and the problems which arise when the experimental information is too limited to properly derive the stability boundary. If validation work has to be done for a specific test case it can be essential to calibrate the N factors for the usage of the transition prediction tools. The necessity of having sufficient experimental transition information for validation purposes available was emphasized.

ACKNOWLEDGEMENTS

This work has partly been carried out within the EUROLIFT II project (European High Lift Programme II) [29]. The EUROLIFT II project is a collaboration between DLR, Airbus-Deutschland, Airbus-France, Airbus-United Kingdom, Alenia Aeronautica, ICAROS Computing, Dassault Aviation, CIRA, ETW, Ing.-Büro Kretschmar, INTA, ONERA, NLR and FOI. The project is managed by DLR and is partly funded by the European Union (Project Ref: GRD-2004-502896).

REFERENCES

- [1] Rudnik, R., Ronzheimer, A., and Schenk, M., „Berechnung von zwei- und dreidimensionalen Hochauftriebskonfigurationen durch Lösung der Navier-Stokes Gleichungen“, *Jahrbuch 1996 - Bd. II der Deutschen Gesellschaft für Luft- und Raumfahrt - Lilienthal-Oberth e.V. (DGLR) – JT 96-104, Deutscher Luft- und Raumfahrtkongress, DGLR-Jahrestagung Sep. 1996*, Dresden, Deutsche Gesellschaft für Luft- und Raumfahrt - Lilienthal-Oberth e.V. (DGLR), Godesberger Allee 70, D-53175 Bonn, Germany, 1996, pp. 717-726.
- [2] Smith, A.M.O., Gamberoni, N., “Transition, Pressure Gradient and Stability Theory“, Douglas Aircraft Company, Long Beach, Calif. Rep. ES 26388, 1956.
- [3] van Ingen, J.L., “A suggested Semi-Empirical Method for the Calculation of the Boundary Layer Transition Region“, University of Delft, Dept. of Aerospace Engineering, Delft, The Netherlands, Rep. VTH-74, 1956.
- [4] Arnal, D., Casalis, G., “Laminar-turbulent transition prediction in three-dimensional flows“, *Progress in Aerospace Sciences*, Vol. 36, 2000, pp. 173-191.
- [5] Radespiel, R., Graage, K., Brodersen, O., “Transition Predictions Using Reynolds-Averaged Navier-Stokes and Linear Stability Analysis Methods“, AIAA Paper 91-1641, 1991.
- [6] Stock, H. W., Haase, W., “A Feasibility Study of e^N Transition Prediction in Navier-Stokes Methods for Airfoils“, *AIAA Journal*, Vol. 37, no. 10, 1999, pp. 1187-1196.
- [7] Horton, H. P., Stock, H. W., “Computation of Compressible, Laminar Boundary Layers on Swept, Tapered Wings“, *Journal of Aircraft*, Vol. 32, 1995, pp. 1402-1405.
- [8] Stock, H. W., Degenhardt, E., “A simplified e^N method for transition prediction in two-dimensional, incompressible boundary layers“, *Zeitung für Flugwissenschaft und Weltraumforschung*, Vol. 13, 1989, pp. 16-30.
- [9] Casalis, G., Arnal, D., “ELFIN II Subtask 2.3: Database method – Development and validation of the simplified method for pure crossflow instability at low speed“, ELFIN II - European Laminar Flow Investigation, Technical Report n° 145, ONERA-CERT, Département d’Études et de Recherches en Aérodynamique (DERAT), R.T. DERAT n° 119/5618.16, December 1996.

- [10] Crouch, J. D., Crouch, I. W. M., Ng, L. L., "Transition Prediction for Three-Dimensional Boundary Layers in Computational Fluid Dynamics Applications", *AIAA Journal*, Vol. 40, no. 8, 2002, pp. 1536-1541.
- [11] Warren, E. S., Hassan, H. A., "Transition Closure Model for Predicting Transition Onset", *Journal of Aircraft*, Vol. 35, 1998, pp. 769-775.
- [12] Czerwiec, R.M., Edwards, J. R., Rumsey, C. L., Bertelrud, A., Hassan, H. A., "Study of High-Lift Configurations Using k- ζ Transition/Turbulence Model", AIAA Paper 99-3186, 1999.
- [13] Edwards, J. R., Roy, C. J., Blottner, F. G., Hassan, H. A., "Development of a One-Equation Transition/Turbulence Model", *AIAA Journal*, Vol. 39, no. 9, 2001, pp. 1691-1698.
- [14] Langtry, R.B., Menter, F.R., "Transition Modeling for General CFD Applications in Aeronautics", AIAA Paper 2004-522, 2005.
- [15] FLOWer - Installation and User Handbook, Release 116, Doc.Nr. MEGAFLOW-1001, Institut für Entwurfsaerodynamik, Deutsches Zentrum für Luft- und Raumfahrt e.V., 2000.
- [16] Krumbein, A., Stock, H. W., "Laminar-turbulent Transition Modeling in Navier-Stokes Solvers using Engineering Methods", ECCOMAS 2000, Barcelona (e), 11.-14. September 2000, *ECCOMAS 2000 - CD-Rom Proceedings*, editor: International Center for Numerical Methods in Engineering (CIMNE), 2000, ISBN: 84-89925-70-4, Depósito Legal: B-37139-2000.
- [17] Krumbein, A., "Coupling of the DLR Navier-Stokes Solver FLOWer with an e^N -Database Method for laminar-turbulent Transition Prediction on Airfoils", *New Results in Numerical and Experimental Fluid Mechanics III*, Notes on Numerical Fluid Mechanics - Vol. 77, Berlin, Heidelberg, New York, Springer Verlag, 2002, pp. 92-99.
- [18] Schrauf, G., "LILLO 2.1 User's Guide and Tutorial", Bremen, Germany, GSSC Technical Report 6, originally issued Sep. 2004, modified for Version 2.1 July 2006.
- [19] Krumbein, A., "Automatic Transition Prediction and Application to High-Lift Multi-Element Configurations", *Journal of Aircraft*, Vol.42, 2005, pp. 1150-1164; also AIAA Paper 2004-2543, June/July 2004.
- [20] Krumbein, A., "Automatic Transition Prediction and Application to 3D Wing Configurations", in print at *Journal of Aircraft*, DOI: 10.2514/2254; also AIAA Paper 2006-914, June 2006.
- [21] Schmitt, V., Charpin, F., "Pressure Distributions on the ONERA-M6-Wing at Transonic Mach Numbers", *AGARD Advisory Report No. 138*, 1979, pp. B1-1 – B1-44.
- [22] Schmitt, V., Cousteix, J., "Étude de la couche limite tridimensionnelle sur une aile en flèche", ONERA, Rapport Technique N° 14/1713 AN, Châtillon, France, July 1975.
- [23] Baldwin, B. S., Lomax, H., "Thin-Layer Approximation and Algebraic Model for Separated Turbulent Flows", AIAA Paper 78-257, 1978.
- [24] Schmidt, G. S., Mueller, Th. J., "Analysis of Low Reynolds Number Separation Bubbles Using Semiempirical Methods", *AIAA Journal*, Vol. 27, No. 8, 1989, pp. 993-1001.
- [25] Stock, H. W., "Infinite Swept-Wing Navier-Stokes Computations with e^N Transition Prediction", *AIAA Journal*, Vol. 43, No. 5, June 2005, pp. 1221-1229.
- [26] Schrauf, G., "Transition Prediction using different Linear Stability Analysis Strategies", AIAA Paper 1994-1848, June 1994.
- [27] Saric, W. S., Reed, H. L., "Toward Practical Laminar Flow Control – Remaining Challenges", AIAA Paper 2004-2311, June 2004.
- [28] Saric, W. S., Reed, H. L., White, E. B., "Stability and Transition of Three-Dimensional Boundary Layers", *Annu. Rev. Fluid. Mech.*, Vol. 35, 2003, pp. 413-440.
- [29] EUROLIFT II-European High Lift Programme II, Annex B: "Description of Work", A Specific Targeted Research Project of the 6th European Framework Program, GRD-2004-502896, 2004.

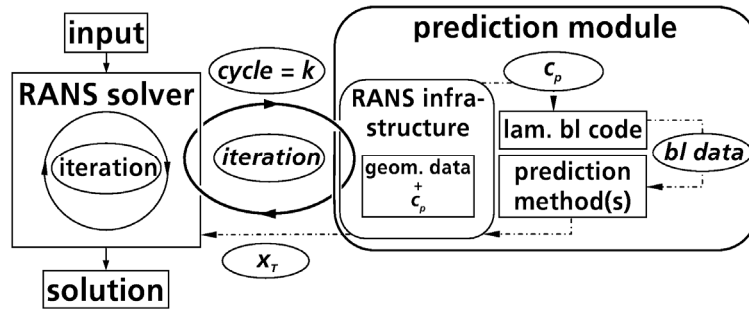


Fig. 1 Coupling structure of the RANS solver and the transition prediction module.

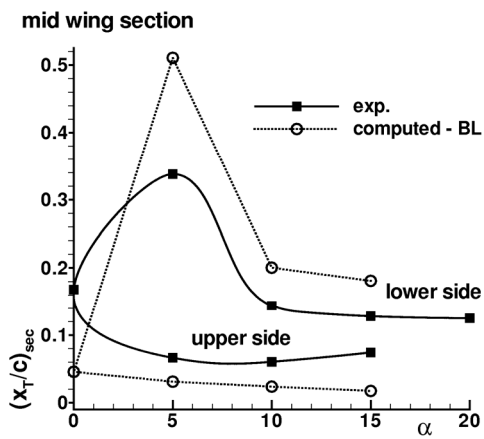


Fig. 2 Computed transition points in the mid wing section of the M6 wing, $N_{TS} = N_{CF} = 6.485$.

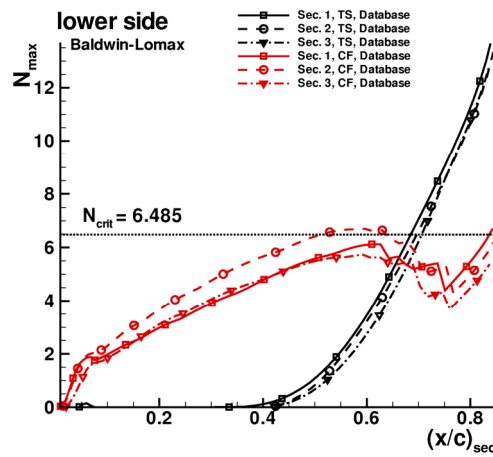


Fig. 3 N factor curves of TS and CF waves for the M6 mid wing section, $\alpha = 5^\circ$, database methods.

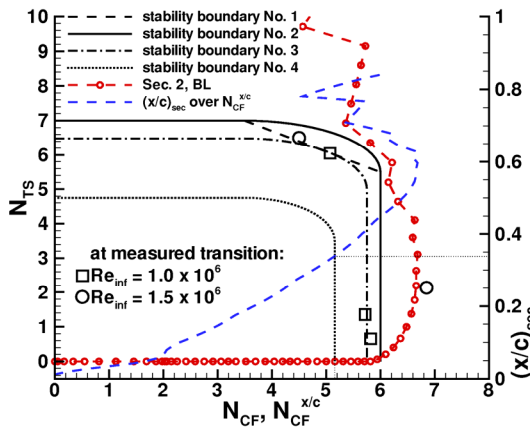


Fig. 4 Different stability boundaries, N_{CF} - N_{TS} curve and $(x/c)_{sec}$ -over- N_{CF} curve of the M6 mid wing section for $\alpha = 5^\circ$.

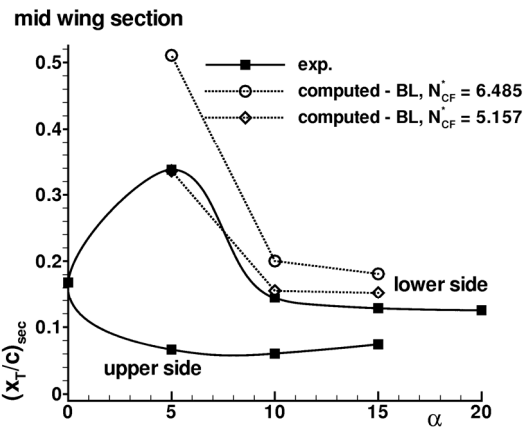


Fig. 5 Computed transition points in the mid wing section of the M6 wing, different values for N_{CF} .

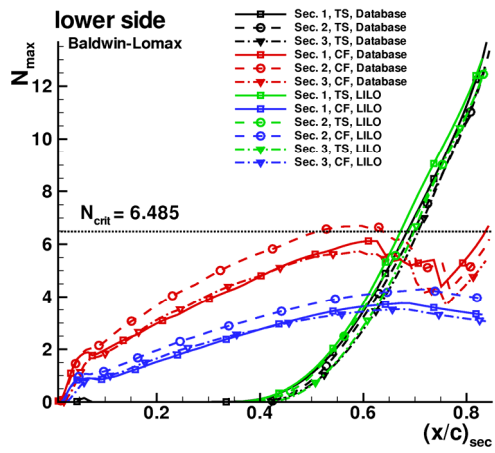


Fig. 6 N factor curves of TS and CF waves for the M6 mid wing section, $\alpha = 5^\circ$, database methods and local, linear stability code LILO.

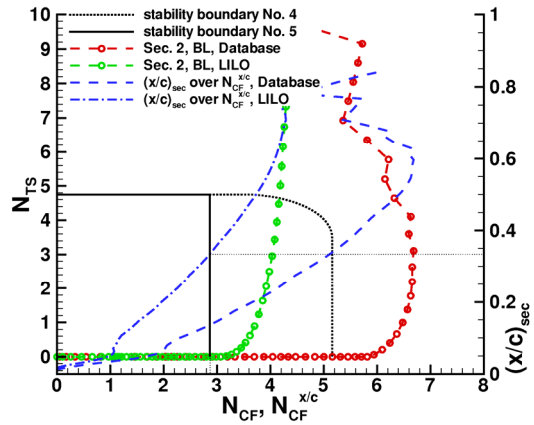


Fig. 7 Different stability boundaries, N_{CF} - N_{TS} curves and $(x/c)_{sec}$ -over- N_{CF} curves of the M6 mid wing section for $\alpha = 5^\circ$, database methods and local, linear stability code LILO.